LEGIBILITY NOTICE

A major purpose of the Technical Information Center is to provide the broadest dissemination possible of information contained in DOE's Research and Development Reports to business, industry, the academic community, and federal, state and local governments.

Although a small portion of this report is not reproducible, it is being made available to expedite the availability of information on the research discussed herein.

LA-UR -89-1664

CONF-8911151--1

Received by OSTI

JUN 07 1989

LA-UR--89-1664

DE89 013453

TITLE CHAOTIC BEHAVIOR IN NONLINEAR POLARIZATION DYNAMICS

AUTHOR(S): Daniel David, CNLS
D. D. Holm, T-7
Michael V. Tratnik, CNLS

SUBMITTED TO Nearly Integrable Systems and Applications. Institute for Mathematics and its Applications, University of Minnesota, Minneapolis - Fall 1988 (November 7-11, 1989)

DISCLAIMER

Los Alamos Los Alamos National Laboratory
Los Alamos, New Mexico 87545

CHAOTIC BEHAVIOR IN NONLINEAR POLARIZATION DYNAMICS

D. David, D.D. Holm, and M.V. Tratnik
C.N.L.S. and Theoretical Division, MS B258
Los Alamos National Laboratory
Los Alamos, NM 87545

Abstract. We analyze the problem of two counterpropagating optical laser beams in a slightly nonlinear medium from the point of view of Hamiltonian systems; the one–beam subproblem is also investigated as a special case. We are interested in these systems as integrable dynamical systems which undergo chaotic behavior under various types of perturbations. The phase space for the two–beam problem is $C^2 \times C^2$ when we restrict to the regime of travelling–wave solutions. We use the method of reduction for Hamiltonian systems invariant under one-parameter symmetry groups to demonstrate that the phase space reduces to the two–sphere S^2 and is therefore completely integrable. The phase portraits of the system are classified and we also determine the bifurcations that modify these portraits; some new degenerate bifurcations are presented in this context. Finally, we introduce various physically relevant perturbations and use the Melnikov method to prove that horseshoe chaos and Arnold diffusion occur as consequences of these perturbations.

1. Introduction. In this paper, we treat optical polarization dynamics for two counterpropagating laser beams (Section 2) in a lossless, cubically nonlinear, Kerr like, parity-invariant, anisotropic homogeneous medium with small nonlinearities (for instance, polarized beams in an optical fiber); the problem of single beam is analyzed in Section 3. Nonlinear effects in polarized light beams have been studied for nearly three decades. For instance, the precession of the polarization ellipse for a beam in a nonlinear medium is demonstrated in Maker *et al.* [1964]. Stable configurations of the nonlinear interaction of two counterpropagating waves in an isotropic medium are studied, e.g., in Kaplan [1983] and Lytel [1984]. Polarization bistability in such a medium and numerical evidence for chaos is found in Otsuka *et al.* [1985] and Gaeta *et al.* [1987]. Interpretations of experimental optical data in terms of chaotic behavior are given in Trillo *et al.* [1986]. Analyses of special cases of the one–beam and two–beam problem appear in Tratnik and Sipe [1987] where the authors give physical interpretations for some of the fixed points and find special solutions. Here we provide a unified study and a complete analysis of the qualitative properties of these problems (phase portraits, bifurcations, special solutions) in the regime of travelling–wave solutions. Hamiltonian techniques are used to reduce the phase space $C^2 \times C^2$ for the travelling–wave dynamics of the two–beam problem and C^2 in the case of the one–beam problem to the spherical surface S^2. Bifurcations of the phase portraits on S^2 are

determined, and homoclinic and heteroclinic orbits connecting hyperbolic fixed points are identified. These orbits are the stable and unstable manifolds of the hyperbolic fixed points and they separate various regions in phase space, each characterized by a different type of periodic behavior. Under spatially periodic perturbations of the medium parameters, these stable and unstable manifolds for the travelling-wave solutions are shown to tangle so as to produce a Smale horseshoe in the Poincaré map of first return induced from the periodic perturbation; Arnold diffusion is also implied for perturbations that break enough of the symmetries of the Hamiltonian function in the two–beam case. The presence of this tangle is diagnosed via the Melnikov method, as generalized to higher than three dimensions in Wiggins [1988]. The location of the chaotic set is characterized analytically, as well as its dependence on the material parameters and the intensities of the optical beams.

2. The Two–Beam Problem.

2.1. Definition and reduction to S^2. The two–beam problem for two counterpropagating travelling optical wave pulses is described by the following Hamiltonian function and equations of motion defined on $C^2 \times C^2$:

$$H = \tfrac{1}{2}\chi^{(3)}_{ijk\ell}(e_i^* e_j e_k e_\ell^* + \bar{e}_i^* \bar{e}_j \bar{e}_k \bar{e}_\ell^* + 4 e_i^* e_j \bar{e}_k \bar{e}_\ell^*) \ , \tag{2.1}$$

$$\{F, G\} = i(\bar{\kappa}/\bar{r})\left(\frac{\partial G}{\partial \mathbf{e}^*}\frac{\partial F}{\partial \mathbf{e}} - \frac{\partial F}{\partial \mathbf{e}^*}\frac{\partial G}{\partial \mathbf{e}}\right) + i(\kappa/r)\left(\frac{\partial G}{\partial \bar{\mathbf{e}}^*}\frac{\partial F}{\partial \bar{\mathbf{e}}} - \frac{\partial F}{\partial \bar{\mathbf{e}}^*}\frac{\partial G}{\partial \bar{\mathbf{e}}}\right) \ , \tag{2.2}$$

$$\frac{\partial e_i}{\partial \tau} = i(\bar{\kappa}/\bar{r})\,\chi^{(3)}_{ijk\ell}(e_j e_k e_\ell^* + 2 e_j \bar{e}_k \bar{e}_\ell^*) \ , \tag{2.3a}$$

$$\frac{\partial \bar{e}_i}{\partial \tau} = i(\kappa/r)\,\chi^{(3)}_{ijk\ell}(\bar{e}_j \bar{e}_k \bar{e}_\ell^* + 2\bar{e}_j e_k e_\ell^*) \ . \tag{2.3b}$$

The Poisson bracket is canonical; as is usual for Hamiltonian systems, the travelling-wave evolution of a dynamical quantity F is determined by $\partial F/\partial \tau = \{F, H\}$, where τ is the travelling-wave variable. In the above equations, the dependent variables $\mathbf{e}$ and $\bar{\mathbf{e}}$ represent the electric field amplitudes associated with each of the beams and both are complex two-vectors taking values in C^2. The quantity $\chi^{(3)}$ is the third order susceptibility tensor parametrizing the nonlinear polarizability of the medium and verifying the involutions $\chi^{(3)}_{ijk\ell} = \chi^{(3)*}_{j i \ell k}$ and $\chi^{(3)}_{ijk\ell} = \chi^{(3)}_{\ell j k i} = \chi^{(3)}_{i k j \ell}$. r and $\bar{r}$ denote the intensities of the two beams, and the constants κ and $\bar{\kappa}$ are related to the group velocities of the beams (see David *et al.* [1989] for details of the problem formulation and background references to the physics literature). A remarkable property of the Hamiltonian function (2.1) is that it is invariant

under a diagonal action of the group $U(1) \times U(1)$. This allows us to use the Marsden-Weinstein reduction procedure for Hamiltonian systems with symmetry (see Marsden and Weinstein [1974]) to show that two consecutive Lie–Poisson maps of $C^2 \times C^2$ reduce the system to the two–sphere S^2.

THEOREM 1. For isotropic media, the Hamiltonian system (1.1–1.3) reduces to a two-dimensional Hamiltonian system on the two-sphere S^2.

We give only a sketch of the proof; again, for more details, see David *et al.* [1989]. The first step of the reduction consists of restricting the phase space $C^2 \times C^2$ to the product manifold $S^2 \times S^2$. This is possible because of the rotational invariances (one in each C^2) of the Hamiltonian function; the conserved quantities associated to these invariances are the intensities of the beams, r and $\bar{r}$, whose level surfaces define submanifolds of the initial phase space in which the motion is confined. (The essence of reduction consists of restricting the phase space to level hypersurfaces of the various conserved quantities of the system.) The first reduction is accomplished in the following manner. We first restrict $C^2 \times C^2$ to the subspace $S^3 \times S^3$ by rewriting the system in terms of bilinear forms in the electric field amplitudes:

$$(\mathbf{e}, \bar{\mathbf{e}}) \longrightarrow (\mathbf{u} = \mathbf{e}^\dagger \vec{\sigma} \mathbf{e}, \bar{\mathbf{u}} = \bar{\mathbf{e}}^\dagger \vec{\sigma} \bar{\mathbf{e}}) \ , \tag{2.4a}$$

with

$$\mathbf{W} = \vec{\sigma}_{ij} \chi^{(3)}_{ijk\ell} \vec{\sigma}_{k\ell} = \mathrm{Diag}(\lambda_1, \lambda_2, \lambda_3) \ , \tag{2.4b}$$

and where $\vec{\sigma}$ represents the three Pauli spin matrices; this representation is sometimes refered to as the *Stokes* representation and each copy of S^2 is known as a Poincaré sphere. The Poincaré sphere provides a convenient way of describing the polarization states of a beam; the north and south poles represent the two opposite circularly polarized states, equatorial points are associated with linearly polarized states, and all other points correspond to elliptically polarized states. It proves convenient to introduce the eigenvalues of $\mathbf{W}$, the λ_i; here we deal with isotropic media, in which case $\lambda_3 = \lambda_1$. The intensities of the beams, r and $\bar{r}$, are the norms of $\mathbf{u}$ and $\bar{\mathbf{u}}$ whose level surfaces form products of two–spheres in $S^3 \times S^3$; these surfaces in fact determine a Hopf fibration of $S^3 \times S^3$ with $S^2 \times S^2$ leaves labeled by the conserved intensities. The motion on $S^2 \times S^2$ is expressible as an evolution system for spherical angles on each sphere:

$$(\mathbf{u}, \bar{\mathbf{u}}) \longrightarrow (\theta, \phi, \bar{\theta}, \bar{\phi}) \ . \tag{2.5}$$

We remark that the passage from $C^2 \times C^2$ to $S^3 \times S^3$ is similar to the passage from the Cayley-Klein parameters to the angular momentum representation for the dynamics of the rigid body. (See, e.g., Crampin and Pirani [1987], pp. 202–207, for a clear discussion of Cayley-Klein parameters.) For isotropic media there exists a further S^1 rotation symmetry of the Hamiltonian function (as in the symmetric rigid body). The associated conserved quantity, σ, is the total projection of the angular momentum (per unit length) of the two beams (as defined below) along the direction of propagation. This symmetry allows us to perform a second reduction step which brings the phase space to a single two-sphere S^2, coordinatized by the angles ψ and α through the following formulas:

$$\begin{aligned} &\alpha = \phi - \overline{\phi}\,, \quad \beta = \phi + \overline{\phi}\,, \quad \sigma = \kappa\cos\theta + \overline{\kappa}\cos\overline{\theta}\,, \\ &\omega(\psi) = \kappa\cos\theta - \overline{\kappa}\cos\overline{\theta} = \omega_o + R\cos\psi\,, \end{aligned} \tag{2.6a}$$

where ω_o and R depend on the value of σ as follows:

$$\begin{aligned} &\sigma \geq |\overline{\kappa}| - |\kappa| : \quad \omega_o = |\kappa| - |\overline{\kappa}|\,, \quad R = |\kappa| + |\overline{\kappa}| - \sigma; \\ &|\kappa| - |\overline{\kappa}| \leq \sigma \leq |\overline{\kappa}| - |\kappa| : \quad \omega_o = -\sigma\,, \quad R = 2|\kappa|; \\ &\sigma \leq |\kappa| - |\overline{\kappa}| : \quad \omega_o = |\overline{\kappa}| - |\kappa|\,, \quad R = |\kappa| + |\overline{\kappa}| + \sigma\,. \end{aligned} \tag{2.6b}$$

Generically, the above choices (2.6b) ensure reduction to a smooth manifold. Special situations arise however when σ is equal in magnitude to $|\kappa| - |\overline{\kappa}|$; for these cases, one of the poles (or both of them if $\sigma = 0, i.e., |\overline{\kappa}| = |\kappa|$), on the sphere becomes a singular point, so that the reduced phase space may be formally identified with $S^2 \backslash P$. We point out that this causes no difficulty for the analysis of the motion; in fact, interesting degenerate bifurcations take place in these singular cases. On S^2, the Hamiltonian function, the Poisson bracket, and the equations of motion become

$$H = \tfrac{1}{2}\lambda_1 \left(r^2 + \overline{r}^2 + (r\overline{r}/\kappa\overline{\kappa})\left[\Gamma\omega^2 + \Delta\sigma^2 + 2E\sigma\omega + f(\psi)\overline{f}(\psi)\cos\alpha\right]\right)\,, \tag{2.7a}$$

$$\{F, G\} = \frac{2\kappa\overline{\kappa}}{r\overline{r}R\sin\psi}\left[\frac{\partial F}{\partial\psi}\frac{\partial G}{\partial\alpha} - \frac{\partial G}{\partial\psi}\frac{\partial F}{\partial\alpha} + 2R\sin\psi\left(\frac{\partial F}{\partial\beta}\frac{\partial G}{\partial\sigma} - \frac{\partial G}{\partial\beta}\frac{\partial F}{\partial\sigma}\right)\right]\,, \tag{2.7b}$$

$$\begin{aligned} &\frac{\partial\psi}{\partial\tau} = -\lambda_1 f(\psi)\overline{f}(\psi)\sin\alpha/R\sin\psi\,, \\ &\frac{\partial\alpha}{\partial\tau} = 2\lambda_1(\Gamma\omega + E\sigma) + \lambda_1\left[(\sigma - \omega)f(\psi)/\overline{f}(\psi) - (\sigma + \omega)\overline{f}(\psi)/f(\psi)\right]\cos\alpha\,, \end{aligned} \tag{2.7c}$$

where ω is given by (2.6a) and

$$\Gamma = \tfrac{1}{4}(L-1)\rho_+ - L\,, \quad \Delta = \tfrac{1}{4}(L-1)\rho_+ + L\,, \quad E = \tfrac{1}{4}(L-1)\rho_-\,, \quad L = \lambda_2/\lambda_1\,,$$

$$\rho_\pm = (r\overline{\kappa}/\overline{r}\kappa \pm \overline{r}\kappa/r\overline{\kappa})\,, \quad f(\psi) = \sqrt{4\kappa^2 - (\sigma+\omega)^2}\,, \quad \overline{f}(\psi) = \sqrt{4\overline{\kappa}^2 - (\sigma-\omega)^2}\,. \tag{2.7d}$$

In addition to (2.7c), there is a quadrature in the variable β:

$$\frac{\partial\beta}{\partial\tau} = 2\lambda_1(\Delta\sigma + E\omega) - \lambda_1\left[(\sigma-\omega)\,f(\psi)/\overline{f}(\psi) + (\sigma+\omega)\,\overline{f}(\psi)/f(\psi)\right]\cos\alpha\,. \tag{2.7e}$$

Since the reduced system is Hamiltonian on a two-dimensional phase space, there immediately follows the

COROLLARY 1. The two-beam system (2.3) is completely integrable.

An important remark is that the reduction procedure just described is not characterized by any loss of information about the solutions. Although the reduced system lives on a lower dimensional subspace of the initial phase space, the full solution may be reconstructed from the reduced solution via quadratures.

THEOREM 2. The solution manifold of the system (2.3) is completely determined by that of the reduced Hamiltonian system on S^2.

Roughly speaking, Theorem 2 is proved by going backwards through the proof of Theorem 1. First, by integrating for β, taking into account that σ is a constant of the motion, and inverting (2.5), we construct the solution on the product space $S^2 \times S^2$ of Poincaré spheres. Next, we invert (2.4a) and use the fact that the intensities of the beams define an immersion in the original phase space; this determines the solution of the initial system up to a phase for each field. These remaining phases are finally reconstructed by substituting into (2.3): this substitution yields quadrature equations for the phases, which may then be integrated to obtain the full solution.

2.2. Fixed points, bifurcations, and special solutions. The reduced system (2.7c) on S^2 for the variables ψ and α exhibits several interesting bifurcations, which take place when certain critical hypersurfaces are crossed in the parameter space. In particular two degenerate bifurcations occur which we call the *Butterfly* bifurcation and the

Teardrop bifurcation. The bifurcations arise when the reduced space S^2 has singularities at either, or both of the poles. These bifurcations involving singular points may be significant from the dynamical point of view as being a possible source of exponentially small (or slow) chaos. To appreciate the various types of bifurcations which occur for the two–beam problem, we begin by determining the set of fixed points (or curves of them), the conditions for their existence, as well as their stability type on the reduced space S^2; these fixed points correspond physically to steady state solutions of the two–beam system (2.3). The parameter spacefor this system is of dimension five (it is, for instance, spanned by Γ, σ, κ, $\overline{\kappa}$, and $\overline{r}/r$) and we could expect rather complex sequences of bifurcations as we travel in the parameter space. Here, we present some sequences that are representative of the global picture (for a more complete picture of the phase portraits and bifurcations that exist for both the one–beam and the two–beam problems, see David *et al.* [1989]).

The most common sequence of portraits with bifurcations is depicted in Figure 1; this sequence is obtained, for instance, by setting $\sigma \neq 0$ and $|\overline{\kappa}|/|\kappa| = 1$, and by varying the remaining parameter Γ. For large absolute values of this parameter, we observe that the phase portrait consists of a figure–eight pattern composed of a saddle point to which are connected two homoclinic loops. These homoclinic loops separate the phase space into three regions in which periodic motion of different types take place; in addition, each region possesses a limit orbit which is a center, i.e., a stable fixed point. The homoclinic loops are formed by coincidence of the stable and unstable manifolds of the hyperbolic unstable fixed point for this integrable case and are objects which will be important later when we discuss the chaotic behavior of the system under perturbations. In the limit as $|\Gamma| \to \infty$, both homoclinic loops deform to the equator which becomes a circle of fixed points. As Γ approaches certain critical values $\Gamma_{\pm}$, the loops collapse together onto the saddle point, at which point a pitchfork bifurcation occurs, after which the phase portrait on S^2 consists of a one–parameter family of periodic orbits with two stable centers.

The second example which we present is the limit of the preceding case when $\sigma = 0$. This situation gives rise to a degenerate bifurcation which we term the *Butterfly* bifurcation and which is illustrated in Figure 2. This bifurcation is characterized by the two centers within the homoclinic loops of the preceding case being located at the poles and these poles *always* remaining fixed points of the system; in fact, these poles are the singular points of the reduced phase space for the case $\sigma = 0$. In contrast with the first case, the

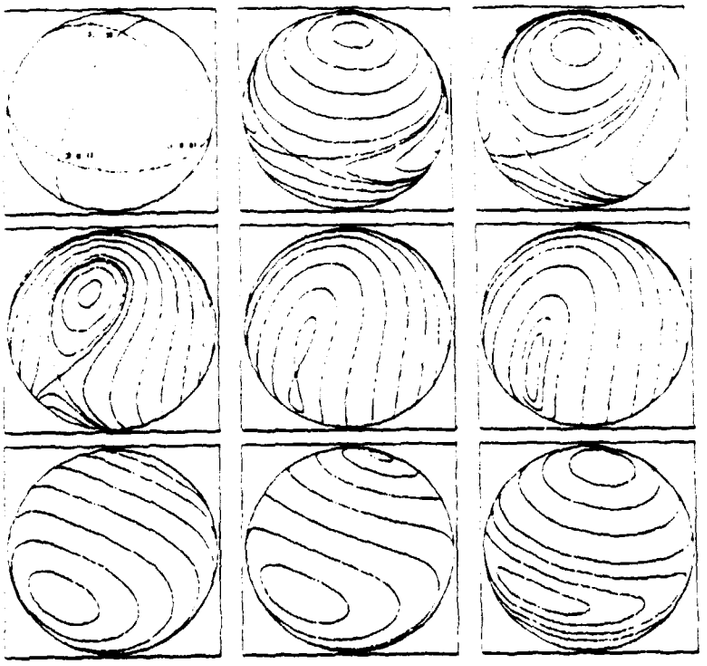

Figure 1. The phase portrait and its pitchfork bifurcations for $\sigma \neq 0$ and $|\overline{\kappa}| = |\kappa|$.

homoclinic loops in this case cannot shrink to the equator because their enclosed centers must remain at the poles. Instead, the homoclinic loops collapse to lines, so that when $\Gamma = \Gamma_+ = -1$ a half-great-circle of fixed points extends from one pole to the other. The bifurcation then proceeds as Γ becomes greater than -1. The half-great-circle opens up into two curves which behave like heteroclinic orbits in all respects. As Γ increases above -1, these heteroclinic orbits rotate azimuthally around the sphere and collide back together in the back of the sphere as $\Gamma = 1$, at which point the bifurcation sequence reverses as the colliding heteroclinic orbits transform, once more, into a figure-eight homoclinic pattern, with the homoclinic point lying on the equator. Figure 3 illustrates the bifurcations in the above two cases in the (Γ, σ)-plane, as Γ is varied at constant σ. The second case, the Butterfly bifurcation, occurs at $\sigma = 0$, along the horizontal (Γ)-axis.

A third case occurs when σ takes its extremal value, equal to the difference of the magnitudes of the kappas. Figure 4 shows the portrait for $\sigma = |\kappa| - |\overline{\kappa}|$; for the opposite case, $\sigma = |\overline{\kappa}| - |\kappa|$, the phase portraits are similar to those in Figure 4, up to exchanging the roles played by the poles. In this case, the north pole is singular. We point out that

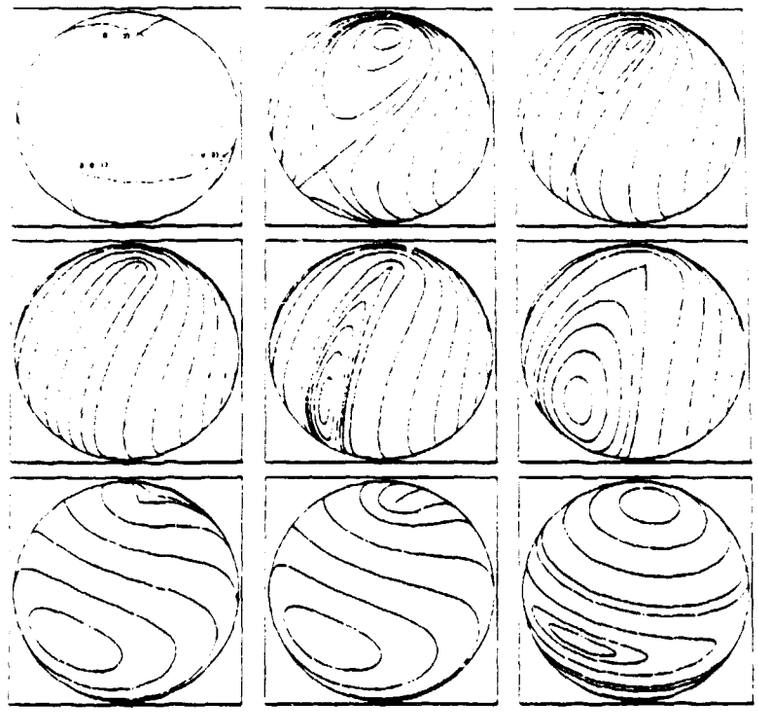

Figure 2. The Butterfly bifurcation occurs when $\sigma = 0$ and $|\overline{\kappa}| = |\kappa|$.
It is degenerate and both poles are singular points on S^2.

the preceding case is a limit of this case also: it is recovered when $|\overline{\kappa}| = |\kappa|$. Here, the portraits are characterized by the occurrence of a degenerate bifurcation which we have termed the *Teardrop* bifurcation. As the pictures show in Figure 4, when $|\Gamma|$ is sufficiently large, the phase portrait contains only periodic orbits. The teardrop bifurcation occurs as $|\Gamma|$ becomes smaller than a certain critical value. As this happens, the north pole develops a singularity and a single homoclinic loop connected to it is created. Note that this contrasts with the usual situation in which homoclinic loops are encountered in pairs; one may also observe that here (as well as in the preceding case) the Euler index of the phase space suddenly jumps from 2 to 1 as this bifurcation occurs, which is another indication of the singular nature of the phase portrait for this case. This homoclinic loop then stretches out, passes through the south pole, and contracts back to a single point at the north pole where the bifurcation "undoes itself," as the pole once more becomes a regular point.

We now present a few examples of special (travelling-wave) solutions of the system (2.3a) and (2.3b), on the Poincaré sphere (for the variables $\mathbf{u}$ and $\overline{\mathbf{u}}$). First, consider

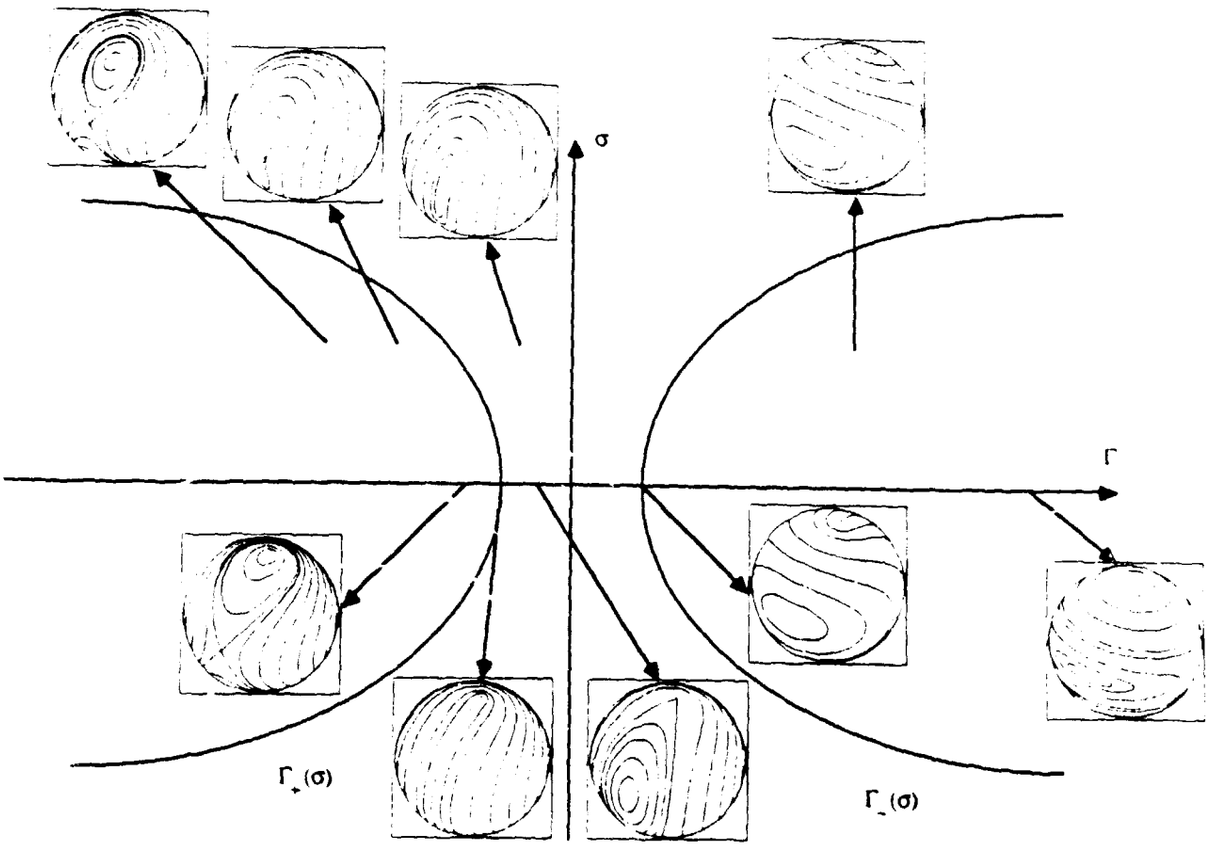

Figure 3. Phase portraits and bifurcations in the (Γ, σ)-plane. Bifurcations occur on the curves $\Gamma_\pm(\sigma)$.

the heteroclinic orbits connecting the poles in Figure 2. The solution u is shown on the left-hand picture in Figure 5. As $\tau \to -\infty$, the beam is circularly polarized. As the travelling-wave variable increases, the solution spirals down from the north pole and the polarization becomes elliptical with increasing eccentricity. At $\tau = 0$, the solution passes through a linear polarization state as the curve crosses the equator. It then proceeds to spiral down, symmetrically to the motion it underwent in the northern hemisphere, towards the south pole where the system asymptotically approaches the other circularly polarized state, opposite to that of the initial state. This solution is reminiscent of a *kink* solution in a completely integrable partial differential equation. As a second example, consider the homoclinic loops in Figure 2. These again give rise to a continuous family of

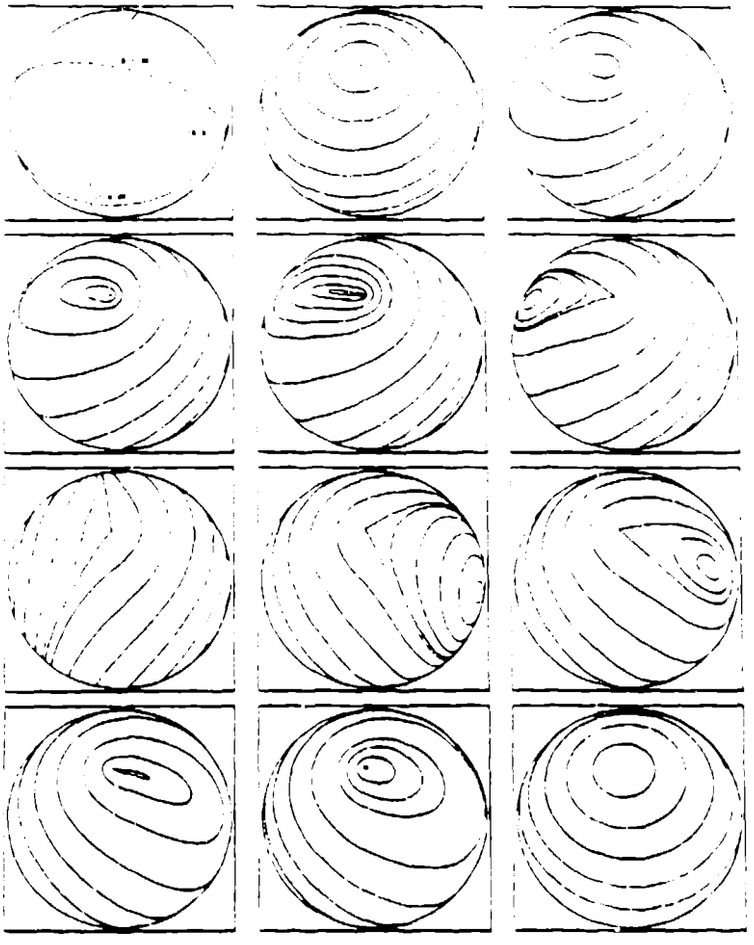

Figure 4. The *Teardrop* bifurcation occurs when $\sigma = |\kappa| - |\overline{\kappa}|$.
A single homoclinic loop is connected to a singular point at the pole.

kink-like travelling-wave solutions with linearly polarized asymptotic states (see middle picture in Figure 5); ***soliton-like*** solutions are also obtained, as a special case when the asymptotic states happen to coincide (see right-hand picture in Figure 5). Notice the existence of a ***winding index***: the solution rotates any number of times around the north pole; each solution is thus characterized by this index as well as its shift in azimuthal linear polarization angle (solitons are those solutions with null shift). The winding index is the integer part of $[\beta(\infty) - \beta(-\infty)]/2\pi$, the number of periods of β, as determined from the quadrature formula (2.7e).

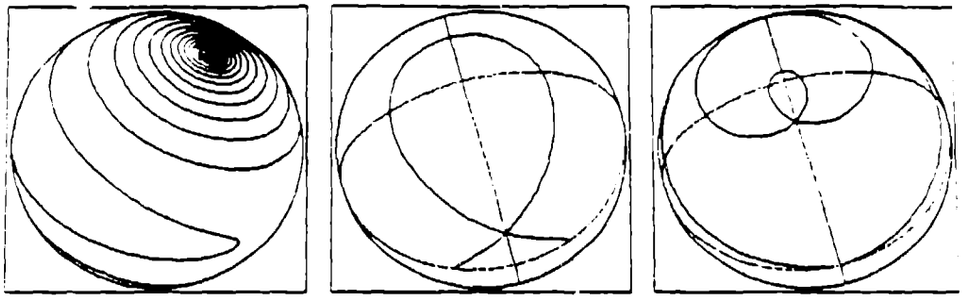

Figure 5. Some kink-like and soliton-like solutions u on the Poincaré sphere.

2.3 Generation of chaotic behavior. Perturbing a completely integrable system which possesses either homoclinic or heteroclinic orbits may yield chaotic dynamics. This is indeed the case for our system, for which the existence of complex dynamics may be analytically demonstrated for certain classes of perturbations. These perturbations are of physical relevance in applied fields such as tele–communications using fiber optics technology and in polarization switching; for instance, periodic perturbations may be created during the manufacturing as twists occuring when the fibers are wound on spools. Here, we specifically report the existence of *Smale horseshoe chaos* for three types of perturbations: first for those perturbations preserving the reduced phase space S^2; then, for constant perturbations breaking the rotational isotropy responsible for the invariance of the total angular momentum σ. In the second case, the phase space for the system returns to $S^2 \times S^2$. Finally, we consider symmetry breaking periodic perturbations, which cause *Arnold diffusion* (see Holmes and Marsden [1982]). The approach we use to demonstrate the existence of these structures is the *Melnikov method*. This method relies on showing that under perturbation the stable and unstable manifolds of a given hyperbolic fixed point intersect transversely. Technically, this is done by calculating the so–called Melnikov function, which is interpretable as a signed measure of the distance separating the stable and unstable manifolds. The form of this Melnikov function depends on the nature of the perturbation; see Wiggins [1988] for details. When the Melnikov function possesses simple zeroes, in the two-dimensional case, the *Poincaré-Birkhoff-Smale theorem* implies that the Poincaré map of first return possesses a horseshoe construction (in higher dimensions,

Arnold diffusion is implied); the horseshoe phenomenon occurs because this Poincaré map produces both a stretching and a folding of the phase points initially near of the hyperbolic point.

We will consider three different perturbations for the two–beam problem, each originating from small deformations of the matrix **W** (see equation (2.4b)) and corresponding to spatially periodic deformations of the nonlinear medium* (optical fiber):

$$\mathbf{W} = \mathrm{Diag}\left(\lambda_1, \lambda_2 + \epsilon\cos\left[\nu(\tau - \tau_0)\right], \lambda_1\right) , \tag{2.8a}$$

$$\mathbf{W} = \mathrm{Diag}\left(\lambda_1 + \epsilon, \lambda_2, \lambda_1\right) , \tag{2.8b}$$

$$\mathbf{W} = \mathrm{Diag}\left(\lambda_1 + \epsilon\cos\left[\nu(\tau - \tau_0)\right], \lambda_2, \lambda_1\right) , \tag{2.8c}$$

where ϵ is a small number. We examine the dynamical consequences of these perturbations on the travelling–wave system for phase points nearby the heteroclinic orbits appearing in the Butterfly bifurcation (see middle row in Figure 2). Perturbations of type (2.8a) preserve S^2 as the phase space. For this two–dimensional case, the Melnikov function is the usual one, i.e., it takes the form of the line integral of the Poisson bracket of the unperturbed H^0 and perturbation H^1 Hamiltonian functions ($H = H^0 + \epsilon H^1$) along the unperturbed heteroclinic orbit:

$$M(\tau_o) = \int_R \left\{H^o, H^1\right\}\left[\omega\left(\tau + \tau_o\right), \alpha(\tau + \tau_o)\right] d\tau , \tag{2.9a}$$

where H^0 is given by (2.7a) and the perturbation Hamiltonian is defined as

$$H^1 = \tfrac{1}{2}\epsilon\left[(r/\kappa)^2(\sigma+\omega)^2 + (\overline{r}/\overline{\kappa})^2(\sigma-\omega)^2 + 4(r\overline{r}/\kappa\overline{\kappa})\left(\sigma^2 - \omega^2\right)\right]\cos(\nu\tau) . \tag{2.9b}$$

The Melnikov integral may be shown to be proportional to $\sin(\nu\tau_0)$; we present a case where it has a simple form, for particular choices of the ratios $\overline{r}/r$ and $\overline{\kappa}/\kappa$:

$$M(\tau_o) = \frac{3r\nu^2\pi}{8\lambda_1^2\sin^2\alpha_o}\,\mathrm{csch}\left[\nu\pi/4\lambda_1 r\sin\alpha_o\right]\sin(\nu\tau_o) , \qquad \overline{r}/r = 1 = -\overline{\kappa}/\kappa , \tag{2.9c}$$

where α_o is defined by $\cos(\alpha_o) = -(1+L)/2$. The existence of simple zeroes of $M(\tau_o)$ yields horseshoe chaos. The type of physical behavior implied by the horseshoe is intermittent

* Should the deformations be quasiperiodic, essentially the same qualitative phenomena will occur. Thus we may think of the perturbations as the dominant spatial frequencies of the deformations.

switching between the two circularly polarization states of the beams; this phenomenon is identifiable with binary symbolic shifts.

Our second type of perturbation, originating from the deformatio : (2.8b), breaks the isotropy responsible for σ–invariance and lifts the reduced phase space to $S^2 \times S^2$. For this second case, the perturbed system falls within category III studied in Wiggins [1988] and the Melnikov integral is expressible as

$$M(\beta_o) = -\int_R \frac{\partial H^1}{\partial \beta}[\omega, \alpha, \sigma, \beta + \beta_o]\, dt \ , \tag{2.10a}$$

where H^1 is given by

$$H^1 = \tfrac{1}{8}\{(\kappa f/r)^2 [1 + \cos(\alpha + \beta)] + (\overline{\kappa}\overline{f}/\overline{r})^2 [1 + \cos(\alpha - \beta)] + (4r\overline{r}/\kappa\overline{\kappa})(\cos\alpha + \cos\beta)\} \ . \tag{2.10b}$$

Choosing the same particular ratios $\overline{r}/r$ and $\overline{\kappa}/\kappa$ as in the case above, we see that the Melnikov function once more adopts a trigonometric form,

$$M(\beta_o) = -\frac{r^2(2 - \cos\alpha_o)\sin\beta_o}{\lambda_1 \sin\alpha_o} \ , \tag{2.10c}$$

and therefore horseshoe chaos is again implied. One distinction from the first perturbation case occurs in the geometry of the stable and unstable manifolds. In this case these manifolds are toroidal objects embedded in $S^2 \times S^2$. For both cases, the phase space is partitioned into stochastic layers separated by invariant tori (or KAM surfaces) which form impenetrable barriers for regions of the polarization state: the polarizations must wander only within these tori.

Perturbations of type (2.8c), in contrast with the other two, yield Arnold diffusion; the phase space is the five–dimensional manifold $S^2 \times S^2 \times R$ and can no longer be partitioned into disconnected chaotic regions: the stochasticity domains form what is called an Arnold's web (or transition chain) and the solution diffuses among the invariant tori. Here again, the perturbed system falls within category III of Wiggins [1988]; however, the Melnikov integral is now a two-component vector function given by

$$M_1(\tau_o, \beta_o) = \int_R \left(\frac{\partial H^0}{\partial \omega}\frac{\partial H^1}{\partial \alpha} - \frac{\partial H^1}{\partial \omega}\frac{\partial H^0}{\partial \alpha} - \frac{\partial H^0}{\partial \sigma}\frac{\partial H^1}{\partial \beta} \right) d\tau + \frac{\partial H^0}{\partial \sigma}\int_R \frac{\partial H^1}{\partial \beta} d\tau \ ,$$

$$M_2(\tau_o, \beta_o) = -\int_R \frac{\partial H^1}{\partial \beta} d\tau \ . \tag{2.11}$$

Integrating for the same ratios $\bar{r}/r$ and $\bar{\kappa}/\kappa$ as before, we find

$$M_1(\tau_o, \beta_o) = \frac{3\nu^2 r\pi\,[(\lambda_2/\lambda_1) - \cos\alpha_o \cos\beta_o]}{16\lambda_1^2 \sin^2\alpha_o} \operatorname{csch}[\nu\pi/4\lambda_1 r \sin\alpha_o] \sin(\nu\tau_o) ,$$

$$M_2(\tau_o, \beta_o) = -\frac{\nu\pi\,[1 - \frac{1}{4}\cos\alpha_o] \sin\beta_o}{4\lambda_1^2 \sin^2\alpha_o} \operatorname{csch}[\nu\pi/4\lambda_1 r \sin\alpha_o] \cos(\nu\tau_o) . \tag{2.12}$$

These functions have two families of simultaneous simple zeroes, whose existence is a necessary condition for the occurrence of Arnold diffusion. Physically, this diffusion means that the polarization state transfers back and forth among the nonlinear modes of the system in an erratic manner.

3. The one–beam problem.

3.1. Definition and reduction to the sphere. We now restrict attention to the problem of a single travelling–wave optical pulse. We introduce the linear and nonlinear susceptibility tensors $\chi^{(1)}$ and $\chi^{(3)}$; far from resonance and in a lossless medium, these tensors are constant, are Hermitian in each $\mathbf{e} - \mathbf{e}^*$ pair, and verify the involutions $\chi^{(3}_{ijk\ell} = \chi^{(3)*}_{j\ell k}$ and $\chi^{(3)}_{ijk\ell} = \chi^{(3)}_{\ell jki} = \chi^{(3)}_{ikj\ell}$ as before. The equations governing the one–beam problem also possess a Hamiltonian formulation. In fact, the Poisson bracket is canonical and the Hamiltonian function and equations of motion are given by

$$H = e_j^* \chi^{(1)}_{jk} e_k + \tfrac{1}{4} e_j^* e_k \chi^{(3)}_{jklm} e_\ell e_m^* , \tag{3.1}$$

$$\frac{\partial e_j}{\partial \tau} = \{e_j, H\} = -i\frac{\partial H}{\partial e_j^*} , \tag{3.2}$$

where τ is the independent variable for travelling waves. As before, $\mathbf{e}$ is a two–component electric field amplitude, i.e., $\mathbf{e}$ takes value in C^2. Furthermore, the beam intensity $r = |\mathbf{e}|^2$ is a conserved quantity.

THEOREM 3. The one-beam problem system (3.2) reduces to a Hamiltonian dynamical system on S^2.

The reduction consists, in effect, in applying the first reduction step that was used for the two–beam problem. The preserved intensity is indeed related to a rotational invariance of the system. Going to the Stokes representation on S^3 coordinatized by $\mathbf{u}$ (defined as

before in (2.4a)), the Hamiltonian function, the Poisson bracket, and the equations of motion become

$$H = \mathbf{b} \cdot \mathbf{u} + \tfrac{1}{2} \cdot \mathbf{W} \cdot \mathbf{u} \tag{3.3}$$

$$\{F, G\}(\mathbf{u}) = \mathbf{u} \cdot \nabla \mathbf{F}(\mathbf{u}) \times \nabla \mathbf{G}(\mathbf{u}) \tag{3.4}$$

$$\frac{d\mathbf{u}}{d\tau} = (\mathbf{b} + \mathbf{W} \cdot \mathbf{u}) \times \mathbf{u} \ , \tag{3.5a}$$

where $\mathbf{W}$ is defined in (2.4b), $\mathbf{b}$ is the birefringence vector,

$$\mathbf{b} = \mathbf{a} + |\mathbf{u}|\mathbf{c} = \mathbf{a} + r\mathbf{c} \ , \tag{3.5b}$$

while $\mathbf{a}$ and $\mathbf{c}$ are constant vectors given by

$$\mathbf{a} = \vec{\sigma}_{kj} \chi^{(1)}_{jk} \ , \qquad \mathbf{c} = \tfrac{1}{2} \vec{\sigma}_{kj} \chi^{(3)}_{jkll} \ , \tag{3.5c}$$

in terms of the susceptibility tensors. Next, changing to spherical coordinates $(u_1, u_2, u_3) = (r \sin\theta \sin\phi, r\cos\theta, r \sin\theta \cos\phi)$ brings the system down to the Poincaré sphere on which the Hamiltonian function, the Poisson bracket, and the equations of motion take the following form:

$$H = \tfrac{1}{2} r^2 \left[(\lambda_1 \sin^2\phi + \lambda_3 \cos^2\phi) \sin^2\theta + \lambda_2 \cos^2\theta \right] \tag{3.6}$$
$$+ r \sin\theta (b_1 \sin\phi + b_3 \cos\phi) + b_2 r \cos\theta \ ,$$

$$\{F, G\} = \frac{1}{r} \left(\frac{\partial F}{\partial \phi} \frac{\partial G}{\partial \cos\theta} - \frac{\partial G}{\partial \phi} \frac{\partial F}{\partial \cos\theta} \right) \ , \tag{3.7}$$

$$\frac{d\theta}{d\tau} = b_1 \cos\phi - b_3 \sin\phi + (\lambda_1 - \lambda_3) r \sin\theta \cos\phi \sin\phi \ , \tag{3.8a}$$

$$\frac{d\phi}{d\tau} = b_2 - (b_1 \sin\phi + b_3 \cos\phi) \cot\theta - r \left(\lambda_1 \sin^2\phi + \lambda_3 \cos^2\phi - \lambda_2 \right) \cos\theta \ . \tag{3.8b}$$

Note that equations (3.8a) and (3.8b) again form a completely integrable system, since it is Hamiltonian on a two-dimensional manifold. Note also that the Poisson bracket (3.7) is the same as that for the system describing the motion of a rigid body; in fact, the rigid body itself is the limit of our system when $\mathbf{b}$ vanishes and the motion equation (3.5a) is the same as for a rigid body with a flywheel attachment.

Before studying the qualitative aspects of the equations (3.8), we mention that in a particular case the system (3.5a) reduces to another well known equation possessing bifurcations to homoclinic orbits. Consider the case when $\mathbf{W}$ is of the form $\mathbf{W} = \omega \mathrm{diag}(1, 1, 2)$

with $\mathbf{b} = (b_1, b_2, 0)$. Eliminating the variables u_1 and u_2 from the equation of motion for u_3 yields a Duffing equation:

$$\begin{aligned} &\frac{d^2u_3}{d\tau^2} = Au_3\left(B - u_3^2\right) , \\ &A = \tfrac{1}{2}\omega^2 , \qquad B = \frac{2H}{\omega} - r^2 - \frac{2\left(b_1^2 + b_2^2\right)}{\omega^2} . \end{aligned} \tag{3.9a}$$

As is well known, when B passes through zero, the solutions of this Duffing equation undergoes a Hamiltonian pitchfork bifurcation to develop homoclinic orbits. As a second example, let $\mathbf{W}$ be as above and $\mathbf{b} = (b_1, 0, b_3)$. Eliminating u_1 and u_2 in the equation of motion for u_3, we obtain:

$$\begin{aligned} &\frac{d^2u_3}{d\tau^2} = A + Bu_3 + Cu_3^2 + Du_3^3 , \\ &A = b_3\left(H - \tfrac{1}{2}\omega r^2\right) , \qquad B = \omega H - \tfrac{1}{2}\omega^2 r^2 - b_1^2 - b_3^2 , \\ &C = -\tfrac{3}{2}\omega b_3 , \qquad D = -\tfrac{1}{2}\omega^2 . \end{aligned} \tag{3.9b}$$

Here, the polarization dynamics reduces to the motion of a particle in a quartic potential, whose solution can be written in terms of elliptic integrals.

3.2. Bifurcation analysis. We now consider the case of a non-parity-invariant material with a C_4 discrete rotation symmetry about the propagation axis; the vector $\mathbf{b}$ then has a single non-null component: $\mathbf{b} = (0, b_2, 0)$, but the eigenvalues λ_i of $\mathbf{W}$ are still arbitrary. Let us also introduce the following parameters:

$$\mu = \lambda_3 - \lambda_1 , \qquad \lambda = (\lambda_2 - \lambda_1)/(\lambda_3 - \lambda_1) , \qquad \beta = b_2/r(\lambda_3 - \lambda_1) . \tag{3.10}$$

The Hamiltonian and the equations of motion become

$$H = \tfrac{1}{2}\mu\left[\left(r^2 - u^2\right)\cos^2\phi + \lambda u^2 + 2\beta r u\right] + \tfrac{1}{2}\lambda_1 r^2 , \tag{3.11}$$

$$\frac{du}{d\tau} = \mu\left(r^2 - u^2\right)\cos\phi\sin\phi , \tag{3.12a}$$

$$\frac{d\phi}{d\tau} = \mu\left[\beta r - \left(\cos^2\phi - \lambda\right)u\right] , \tag{3.12b}$$

where $u = r\cos\theta$. The fixed points for (3.12) are easily determined and classified, using standard techniques; we list them in the following table:

Fixed Point	Coordinates	Constraint	Saddle	Center
F	$\phi = 0 \quad \cos\theta = \beta/(1-\lambda)$	$\beta^2 < (1-\lambda)^2$	$\lambda > 1$	$\lambda < 1$
B	$\phi = \pi \quad \cos\theta = \beta/(1-\lambda)$			
L	$\phi = \pi/2 \quad \cos\theta = -\beta/\lambda$	$\beta^2 < \lambda^2$	$\lambda < 0$	$\lambda > 0$
R	$\phi = -\pi/2 \quad \cos\theta = -\beta/\lambda$			
N	$\cos^2\phi = \lambda + \beta \quad \theta = 0$	———	$0 < \lambda + \beta < 1$	$\lambda + \beta \notin (0,1)$
S	$\cos^2\phi = \lambda - \beta \quad \theta = \pi$	———	$0 < \lambda - \beta < 1$	$\lambda - \beta \notin (0,1)$

Table. The fixed points of system (3.12) and their types.

The above classification is valid only for $\mu \neq 0$. For $\mu = 0$, i.e., when $\lambda_3 = \lambda_1$, the right-hand side of (3.12a) vanishes identically so that the set of fixed points is the circle $\cos\theta = b_2/r(\lambda_2 - \lambda_1) = \beta/\lambda$. The phase portrait depends on two essential parameters, λ and β, or equivalently, $\lambda_2 - \lambda_1$ and b_2/r. Bifurcations take place when the inequalities in the constraint column of the Table become equalities. Thus, the pairs of fixed points (F,B) and (L,R) appear or vanish as the lines $\beta = \pm(1-\lambda)$ and $\beta = \pm\lambda$ are crossed in the (λ, β) parameter plane; see Figure 6.

This parameter plane is partitioned into nine distinct regions separated by four critical lines that intersect at four points. Typical phase portraits corresponding to each of these regions are depicted in Figure 7.

We note that the portraits are invariant under the following discrete transformation:

$$\begin{aligned}
&\phi \longrightarrow \phi \pm \pi \ ; \\
&\phi \longrightarrow \phi \pm \pi, \theta \longrightarrow \pi - \theta, \beta \longrightarrow -\beta \ ; \\
&\phi \longrightarrow \phi \pm \pi/2, \lambda \longrightarrow 1 - \lambda, \beta \longrightarrow -\beta \ ; \\
&\phi \longrightarrow \phi \pm \pi/2, \lambda \longrightarrow 1 - \lambda, \theta \longrightarrow \pi - \theta \ .
\end{aligned} \tag{3.13}$$

Hence, a complete knowledge of the phase portrait necessitates only the study of the quarter plane ($\lambda \leq 1/2, \beta \geq 0$), i.e., of regions 1, 2, 4, and 5. The λ-axis ($\beta = 0$) is a special line; in this limit, we recover the equations of motion for the rigid body, as is easily seen from equation (3.5a). On this axis, the phase portraits themselves are special,

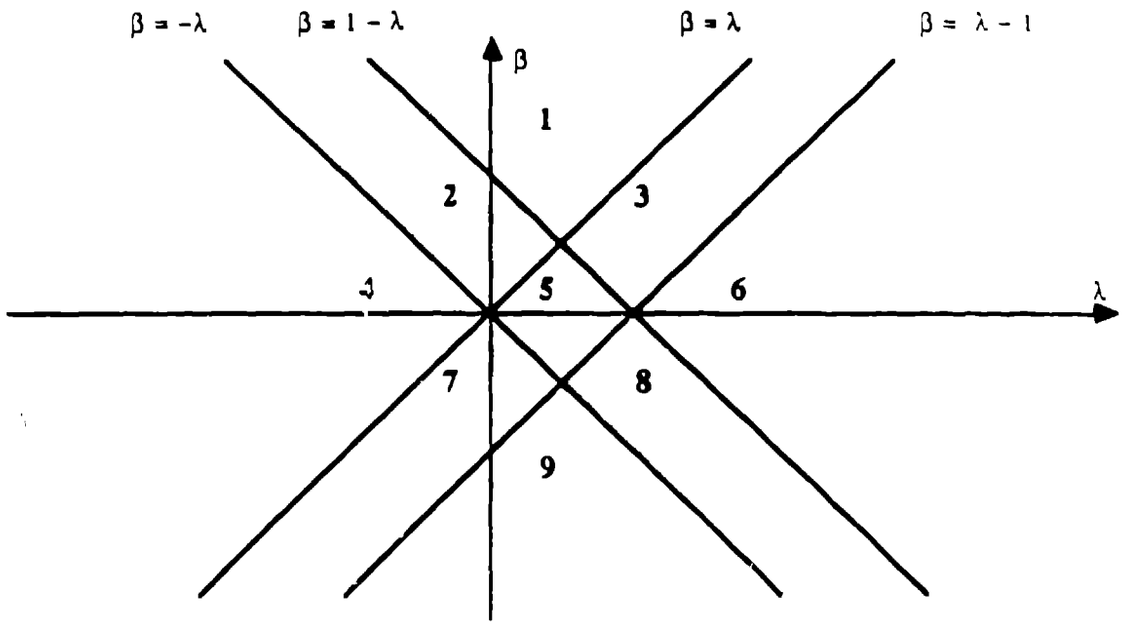

Figure 6. The parameter plane and its bifurcation lines.

although no bifurcations occur (except at $\lambda = 0$ and $\lambda = 1$). For instance, consider region 5. The phase portrait then consists of saddle points at the poles, each of which is connected to a pair of homoclinic loops. When β vanishes these two pairs of loops merge together to form four heteroclinic orbits. Thus, on the whole of the λ-axis, we recover the portrait for the rigid body. Indeed, the portrait consists of the fixed points N and S at the poles and of four other ones are distributed on the equator with azimuthal angles $\phi = 0\ (F), \pi/2\ (R), \pi\ (B),\ 3\pi/2\ (L)$. Two of these are unstable while the other four are stable centers. Which pair is unstable is decided by the value of $\lambda = (\lambda_2 - \lambda_1)/(\lambda_3 - \lambda_1)$: (F,B) are hyperbolic when $\lambda < 0$, (N,S) are hyperbolic when $0 < \lambda < 1$, and (R,L) are hyperbolic when $\lambda > 1$; in each case, the unstable direction is specified by the λ_i which is neither the least nor the greatest among the three.

Remark: Bifurcations taking place as the intensity of the beam is varied occur along vertical lines in the parameter plane, and consist mainly of standard pitchfork bifurcations.

3.3. Homoclinic chaos. We now consider spatially periodic modulations of either the circular-circular polarization self-interaction coefficient λ_2, or the optical activity term

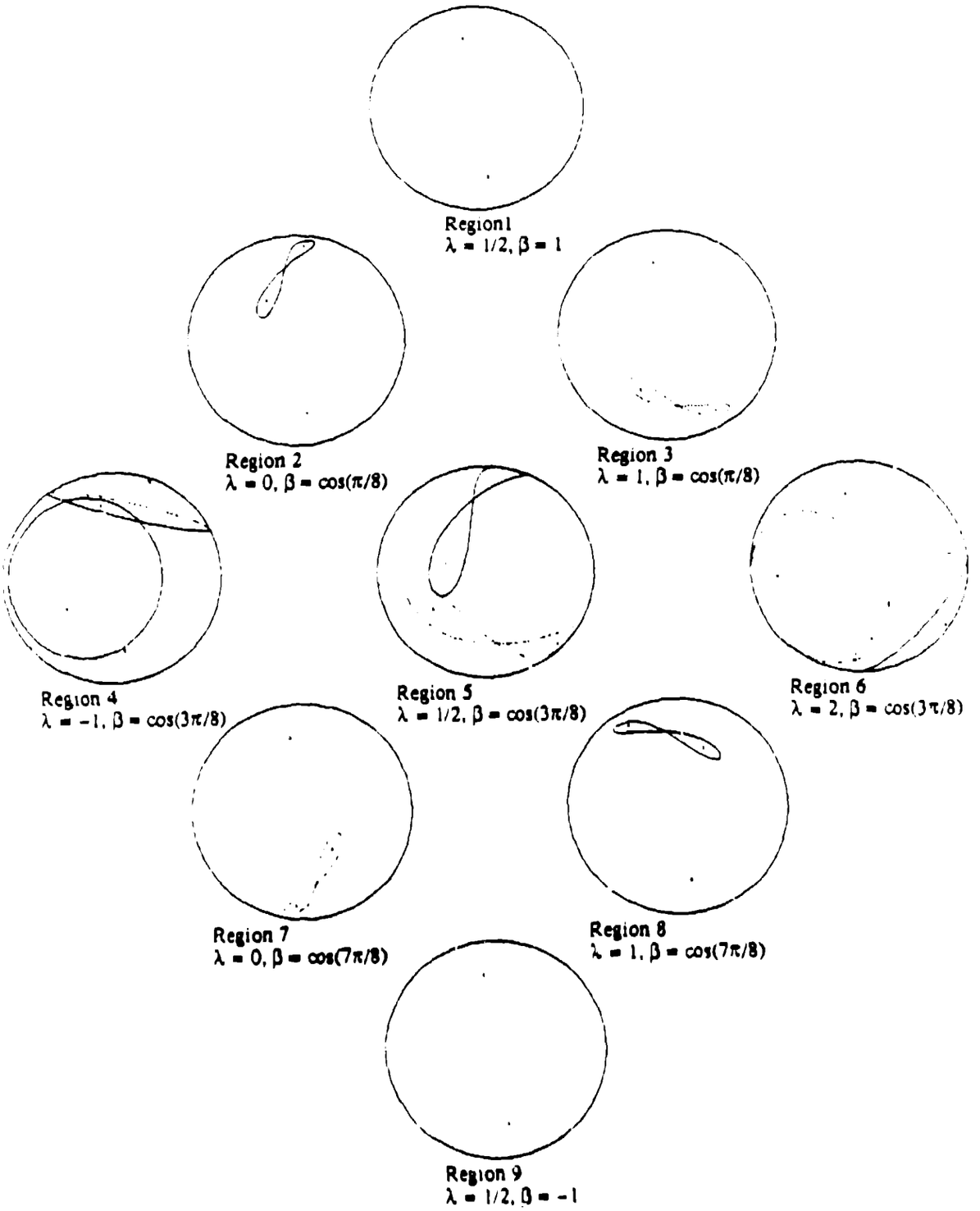

Figure 7. Phase portraits of system (3.12)

b_2. In each case, when the unperturbed medium satisfies the additional condition $\lambda_3 = \lambda_1$, the Melnikov technique leads to an analytically tractable integral for the Melnikov function. In this way, we are able to predict horseshoe chaos in the dynamics of the single, travelling-wave Stokes pulse. We concentrate on the north pole $u = 1$, $\phi = \phi_0$, with $\cos^2\phi_0 = \lambda + \beta$, and evaluate the conserved Hamiltonian at this point to find a relation between u and ϕ the homoclinic orbit:

$$u = -r - 2b_2/\mu\,(\cos^2\phi - \lambda) \tag{3.14}$$

Substituting this expression into the equation of motion for ϕ and integrating produces an explicit expression for the homoclinic orbit:

$$\begin{gathered}\tan\phi = \tan\phi_o/\tanh(\zeta\tau)\,, \qquad \zeta = \tfrac{1}{2}\mu r\sin(2\phi_o)\,, \\ u = -r - \frac{2b_2\left[1 - \cos^2\phi_o\operatorname{sech}^2(\zeta\tau)\right]}{\mu\{\cos^2\phi_o\tanh^2(\zeta\tau) - \lambda\left[1 - \cos^2\phi_o\operatorname{sech}^2(\zeta\tau)\right]\}}\,.\end{gathered} \tag{3.15}$$

We consider a periodic perturbation in the form

$$\lambda_2' = \lambda_2 + \epsilon_1\cos(\nu z)\,, \qquad b_2' = b_2 + \epsilon_2\cos(\nu z)\,, \tag{3.16}$$

where $\epsilon_{1,2} \ll 1$ and ν is the spatial modulation frequency. The perturbation Hamiltonian is

$$H^1 = \tfrac{1}{2}u\,(\epsilon_1 u + 2\epsilon_2)\cos(\nu z)\,, \tag{3.17}$$

from which we calculate the Poisson bracket for the Melnikov integrand,

$$\{H^0, H^1\} = -\mu\sin\phi\cos\phi\,(r^2 - u^2)\,u\cos(\nu z)\,. \tag{3.18}$$

In the particular case $\lambda_2 = \lambda_3$, we find that the Melnikov function (formally the integral of (3.18)) is given by

$$M(\tau_o) = \frac{2\pi\nu^2}{b_2^2}\left\{r\,(\epsilon_1 r + \epsilon_2) \mp \tfrac{1}{2}\epsilon_1 r^2\left[\cos^2\phi_o + (\nu/2b_2)^2\right]\right\}\operatorname{csch}\left[\nu\pi/\mu r\sin(2\phi_o)\right]\sin(\nu\tau_o)\,. \tag{3.19}$$

As a function of τ_0 (which is proportional to the time, t) this expression clearly has simple zeroes, implying horseshoe chaos. As usual, this means that a region near the homoclinic point, under the iteration of the Poincaré map, is stretched, folded, and mapped back into itself. That is, a Smale horseshoe is created. As this horseshoe folds and

refolds, a rectangular region initially nearby the homoclinic point develops into a Cantor set structure whose associated Poincaré map can be shown to contain countably many periodic motions, and uncountably many unstable nonperiodic motions. Physically, this motion corresponds to a (practically unpredictable) meandering of the polarization state as the beam propagates as a travelling-wave.

4. Conclusion. We have presented a dynamical system analysis for two optical systems describing the propagation of either a single beam, or two interacting and counterpropagating beams. The physical interpretation of chaos for several types of spatially periodic perturbations for the two–beam problem is discussed in Section 2. For the one–beam problem we have discussed, horseshoe chaos corresponds to a sort of meandering of the polarization state, that is, an intermittent switching from one elliptical polarization state to a second one whose semi–major axis is approximately orthogonal to that of the first state. The transition between these two states is characterized by a passage nearby the circular state of polarization, once during each switch. This intermittency is realized on the Poincaré sphere by an orbit which spends most of its time near the unperturbed *figure eight* formation with a homoclinic crossing at the north pole (circular polarization) in Figure 7. Under the periodic perturbations of $\mathbf{W}$ or b_2 in (3.1b) this orbit switches deterministically, but with extreme sensitivity to the initial conditions, from one lobe of the figure eight to the other one each time it returns within the crossing region nearby the north pole where the homoclinic tangle is located.

From considerations of the special case in which the Duffing equation (3.9) appears, one could have expected homoclinic chaos to develop for the one–beam problem of nonlinear optical polarization dynamics; indeed, a related special case is studied numerically in Wabnitz [1987]. As opposed to such numerical studies, our analytical approach explores the bifurcations available to the polarization dynamics for both the one–beam and the two–beam problems under the full range of material parameter variations, demonstrates that the horseshoe construct is the mechanism driving the chaotic behavior, and characterizes the location of the chaotic set, or stochastic layer. In some of the cases under consideration, this layer is bounded by KAM curves on the Poincaré sphere, inside of which the travelling-wave dynamics is regular and orbitally stable; higher dimensional chaos also occurs for the two–beam problem in the form of Arnold diffusion.

The strong dependence on the intensities of the beams in the travelling-wave phase

portraits indicates that control and predictability of optical polarization in nonlinear media may become an important issue for future research. In particular, the sensitive dependence on initial conditions found here to be induced by periodic spatial deformations may have implications for the control of optical polarization switching in birefringent media. For instance, an input–output polarization experiment performed with input conditions lying in the stochastic layer for some set of material and beam parameters would show essentially random output after sufficient propagation length, depending on the amplitude and wavelength of the material inhomogeneities and the type of material used.

Acknowledgements. The authors are grateful to the University of Minnesota Institute for Mathematics and its Applications, where this article was written, and to D. Kaup, Y. Kodama, and A.V. Mikhailov for their scientific comments on this work.

References.

M. Crampin and F.A.E. Pirani [1987], *Applicable Differential Geometry*, London Mathematical Society Lecture Notes Series **59**, Cambridge University Press, Cambridge (U.K.).

D. David, D.D. Holm, and M.V. Tratnik [1989], *Hamiltonian chaos in nonlinear optical polarization dynamics*, Physics Reports (to appear).

P.J. Holmes and J.E. Marsden [1982], *Melnikov method and Arnold diffusion for perturbations of integrable Hamiltonian systems*, J. Math. Phys. **23**, 669–675.

A.E. Kaplan [1983], *Light-induced nonreprocity, field invariants, and nonlinear eigenpolarizations*, Opt. Lett. **8**, 560–562.

R. Lytel [1984], *Optical multistability in collinear degenerate four-wave mixing*, J. Opt. Soc. Am. **B1**, 91–94.

P.D. Maker, R.W. Terhune, and C.M. Savage [1964], *Intensity-dependent changes in the refractive index of liquids*, Phys. Rev. Lett. **12**, 507–509.

J.E. Marsden and A. Weinstein [1974], *Reduction of symplectic manifolds with symmetry*, Rep. Math. Phys. **5**, 121–130.

K. Otsuka, J. Yumoto, and J.J. Song [1985], *Optical bistability based on self-induced polarization-state change in anisotropic Kerr-like media*, Opt. Lett. **10**, 508–510.

M.V. Tratnik and J.E. Sipe [1987], *Nonlinear polarization dynamics. I. The single-pulse equations*, Phys. Rev. **A35**, 296 -2975; *II. Counterpropagating beam equations: new simple solutions and the possiblity for chaos*, Phys. Rev. **A35**, 2976–2988; *III. Spatial polarization chaos in counterpropagating beams*, Phys. Rev. **A36**, 4817–4822.

S. Wabnitz [1987], *Spatial chaos in the polarization for a birefringent optical fiber with periodic coupling*, Phys. Rev. Lett. **58**, 1415–1418.

S. Wiggins [1988], *Global Bifurcations and Chaos - Analytical Methods*, Applied Mathematical Sciences **73**, Springer–Verlag, New York.